

Detection of Nonlocal Spin Entanglement by Light Emission from a Superconducting p-n Junction

Alexander Schroer¹ and Patrik Recher^{1,2}

¹*Institut für Mathematische Physik, Technische Universität Braunschweig, D-38106 Braunschweig, Germany*

²*Laboratory for Emerging Nanometrology Braunschweig, D-38106 Braunschweig, Germany*

We model a superconducting p-n junction in which the n- and the p-sides are contacted through two optical quantum dots (QDs), each embedded into a photonic nanocavity. Whenever a Cooper pair is transferred from the n-side to the p-side, two photons are emitted. When the two electrons of a Cooper pair are transported through different QDs, polarization-entangled photons are created, provided that the Cooper pairs retain their spin singlet character while being spatially separated on the two QDs. We show that a CHSH Bell-type measurement is able to detect the entanglement of the photons over a broad range of microscopic parameters, even in the presence of parasitic processes and imperfections.

PACS numbers: 73.40.Lg, 74.45.+c, 42.50.Pq, 03.65.Ud

Quantum entanglement is a resource for quantum computers and quantum communication protocols [1]. For massive particles like electrons, spin entanglement could be created exploiting superconductors (SCs) [2] and crossed Andreev reflection (CAR) [3, 4]. Splitting a Cooper pair (CP) into spatially separated normal leads has been investigated in detail theoretically [5–12] and realized experimentally [13–16]. However, detecting the spin entanglement of the separated electrons remains an open challenge. Different detection schemes have been proposed which are either based on the violation of a Bell inequality using current cross-correlation (noise) measurements [17–23], spin-filtered current measurements [24], or exploiting the statistical [25–33] and many-body [34] properties of electronic beam splitters. All of these proposals, however, are much more involved than the detection of polarization-entangled optical photons, which has been demonstrated successfully [35–37] by violating a Bell inequality [38, 39]. Quite naturally, the question arises if superconductivity and optics can be combined. It has been discussed that p-n junctions in contact with superconductors can exhibit enhanced radiation intensity [40, 41] with experimental demonstration [42], pairwise (entangled) emission of light [43–47], Josephson radiation at optical frequencies [44], squeezed light [46] and laser effects [48–50]. Here, we would like to go a step further and ask the question whether nonlocal spin entanglement can be mapped to optical photons in a superconducting p-n junction. Existing theoretical proposals use the optical recombination of electron and hole singlets in a tunnel-coupled double quantum dot (QD) [51], transfer of spin-entangled electrons into two empty optical quantum dots [52], and the simultaneous transport of spin-entangled electrons and holes into two optical quantum dots embedded in nanocavities [53]. Very recently, the conversion of CPs into photons by laser excitation [54] has also been studied.

In this Letter, we investigate a superconducting p-n junction, where n- and p-sides are contacted via a dou-

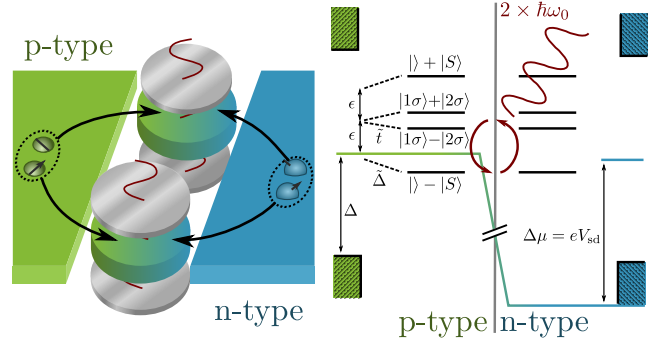


FIG. 1. Left: two QDs (1,2) are tunnel-coupled to superconducting p-type and n-type leads. With a sufficiently large Coulomb repulsion on the QDs, the electrons or holes of incoming CPs are split, such that each QD contains one electron and one hole. Upon recombination polarization-entangled photons are emitted into two nanocavities (gray) with resonance frequency ω_0 and detected by an optical Bell test. Right: Lowest relevant energy levels of the n and p double QD systems. The SC leads hybridize the empty state and the singlet state, $|\pm\rangle|S\rangle$, and the singly occupied states, $|1\sigma\rangle \pm |2\sigma\rangle$, creating a closed two-photon emission cycle.

ble QD structure off-resonantly embedded into two photonic nanocavities (Fig. 1). Due to the superconducting pairing, the QDs are populated with spin-entangled hole pairs and spin-entangled electron pairs, which, upon recombination, emit pairs of polarization-entangled optical photons. Processes which leave behind quasiparticle excitations in the QDs or in the SC leads are suppressed by a sufficiently narrow spectral width of the cavities and thus photons are produced only in pairs with a simultaneous transport of a CP through the device. We show that the photons emitted from the cavities violate a CHSH Bell inequality when CAR is finite, i.e., when the two electrons or holes of a CP retain their spin entanglement when split. We take into account parasitic processes in which two photons are emitted into the same cavity [arising either from sequential emission after elastic cotunneling

(ECT) between the QDs or from imperfect splitting], and show within a microscopic model that entanglement can be detected nevertheless over a broad range of realistic parameters.

Photonic model.—We start with an intuitive effective model for the photons in the two cavities that will be derived formally later on,

$$H_{\text{ph}} = \sum_{i\xi} \hbar\omega a_{i\xi}^\dagger a_{i\xi} + t_{\text{ph}} a_{i\xi}^\dagger a_{\bar{i}\xi} + \left(\frac{\Delta_{\text{ph}}}{2} a_{i\xi} a_{\bar{i}\xi} + \frac{\Lambda_{\text{ph}}}{2} a_{i\xi} a_{i\bar{\xi}} + \text{h.c.} \right), \quad (1)$$

where $a_{i\xi}$ annihilates a photon with circular polarization $\xi = R, L$ in cavity $i = 1, 2$ with mode energy $\hbar\omega$ (counted from the source-drain bias eV_{sd}). Because the cavities are coupled to the superconducting QDs, there is a finite amplitude Δ_{ph} to inject a *nonlocal* photon pair into different cavities i and \bar{i} and an amplitude Λ_{ph} to inject a pair *locally* into the same cavity. Because the pairs can be traced back to one electron singlet and one hole singlet, they always come with opposite polarizations ξ and $\bar{\xi}$. We can choose Δ_{ph} and Λ_{ph} real since they share the same phase factor. There may also be an intercavity coupling t_{ph} mediated by coupling of the QDs via the SC leads. In the absence of magnetic fields, t_{ph} , too, is real. We note that Eq. (1) is meaningful only if $|\omega \pm t_{\text{ph}}| > |\Delta_{\text{ph}} \pm \Lambda_{\text{ph}}|$. This is fulfilled in the off-resonant regime, where $|\omega|$ is large compared to the other parameters in Eq. (1).

A generalized Bogoliubov transformation to the new bosonic fields $\pi_{\mu\nu} = [u_\nu(a_{1\mu}^\dagger + \nu a_{2\mu}^\dagger) + v_\nu(\nu a_{1\bar{\mu}} + a_{2\bar{\mu}})]/(v_\nu^2 - |u_\nu|^2)^{1/2}$ with $u_\pm = \Delta_{\text{ph}} \pm \Lambda_{\text{ph}}$ and $v_\pm = (\hbar\omega \pm t_{\text{ph}}) + \sqrt{(\hbar\omega \pm t_{\text{ph}})^2 - |\Delta_{\text{ph}} \pm \Lambda_{\text{ph}}|^2}$ diagonalizes the Hamiltonian (1), such that

$$H_{\text{ph}} = \sum_{\mu\nu} E_\nu \pi_{\mu\nu}^\dagger \pi_{\mu\nu}, \quad (2)$$

where $E_\pm = \sqrt{(\hbar\omega \pm t_{\text{ph}})^2 - |\Delta_{\text{ph}} \pm \Lambda_{\text{ph}}|^2}$. The ground state $|G\rangle$ is fixed by the condition $\pi_{\mu\nu} |G\rangle = 0$ for all μ, ν . In terms of the original photons this implies

$$|G\rangle = \frac{1}{v_+ v_-} \exp \left[-\frac{1}{2} \left(\frac{u_+}{v_+} - \frac{u_-}{v_-} \right) (a_{1R}^\dagger a_{1L}^\dagger + a_{2R}^\dagger a_{2L}^\dagger) - \frac{1}{2} \left(\frac{u_+}{v_+} + \frac{u_-}{v_-} \right) (a_{1R}^\dagger a_{2L}^\dagger + a_{1L}^\dagger a_{2R}^\dagger) \right] | \rangle, \quad (3)$$

where $| \rangle$ denotes the photonic vacuum. The ground state (3) is a squeezed state [55] of local and nonlocal entangled photon pairs. At low temperatures and with a sufficiently high cavity quality factor, $|G\rangle$ is the dominant contribution to the photonic density matrix.

Photon detection and Bell test.—We use a positive operator valued measure to model the photon detection. The probability to detect at least one photon in cavity i with polarization ξ if $n_{i\xi}$ photons are present, is

given by $P_{i\xi}^+ = 1 - (1 - \gamma)^{n_{i\xi}}$, where $\gamma \in [0, 1]$ is the detection efficiency. With probability $P_{i\xi}^- = 1 - P_{i\xi}^+$, no photon is detected [56]. More generally, a photon with the arbitrary polarization α is detected with probability $P_{i\alpha}^+ = 1 - (1 - \gamma)^{\tilde{a}_{iR}^\dagger \tilde{a}_{iR}}$, where $\tilde{a}_{1R} = a_{1R} \cos \alpha - a_{1L} \sin \alpha$ and $\tilde{a}_{1L} = a_{1R} \sin \alpha + a_{1L} \cos \alpha$.

As a measure of entanglement we employ a CHSH-type Bell inequality. We define four observables A_1 , B_1 , C_2 and D_2 with measurement outcomes ± 1 , where the subscript indicates in which cavity the operator acts. The quantity $\mathcal{B} = A_1 C_2 + A_1 D_2 + B_1 C_2 - B_1 D_2 = A_1(C_2 + D_2) + B_1(C_2 - D_2)$ can take the values ± 2 and hence the expectation value $\langle \mathcal{B} \rangle$ lies within $[-2, 2]$, provided that the observables A_1 to D_2 have definite values independent of any measurement [39]. We adopt the following scheme: $A_1 \equiv A_1^\dagger$ is $(-)$ 1 if only photons with polarization $\alpha(+\pi/2)$ are detected in cavity 1. B_1 is the same measurement rotated by 45° , i.e., $B_1 \equiv B_1^\dagger = A_1^{\alpha+\pi/4}$. Likewise C_2^β and D_2^β measure the photons in cavity 2. Inconclusive events, in which no photons, or photons of both polarizations are detected on one side, are discarded. With the nonlocal correlations $\mathcal{C}(\alpha, \beta) = \sum_{\mu\nu} \mu\nu P_{\alpha\beta}^{\mu\nu} / \sum_{\mu\nu} P_{\alpha\beta}^{\mu\nu}$ the Bell parameter can be expressed as

$$\mathcal{B}_\alpha = \mathcal{C}(0, \alpha) + \mathcal{C}(0, \alpha + \frac{\pi}{4}) + \mathcal{C}(\frac{\pi}{4}, \alpha) - \mathcal{C}(\frac{\pi}{4}, \alpha + \frac{\pi}{4}). \quad (4)$$

In this notation, $P_{\alpha\beta}^{\mu\nu}$ is the probability to obtain the measurement result μ at cavity 1 when polarization detector 1 is set to the angle α and to obtain simultaneously the measurement result ν at cavity 2 when polarization detector 2 is set to the angle β . In an experiment, the probabilities are directly accessible by counting the respective coincidence events. Formally, they are $P_{\alpha\beta}^{\mu\nu} = \langle G | P_{1\alpha}^\mu P_{1\alpha+\pi/2}^\mu P_{2\beta}^\nu P_{2\beta+\pi/2}^\nu | G \rangle$. Owing to the structure of the ground state, the probabilities can be calculated to arbitrary precision, cf. Supplemental Material [57], by finding the eigenvalues of a 4×4 matrix [56].

For a given set of parameters ω , t_{ph} , Δ_{ph} and Λ_{ph} , the Bell test is conclusive only if there are angles α , at which $|\mathcal{B}_\alpha| > 2$. By inspection we find that, like in the two-photon case, \mathcal{B} always takes its maximum for $\alpha = \frac{3\pi}{8}$. The maximum value $\mathcal{B}_{\text{max}} := \max_\alpha |\mathcal{B}_\alpha|$ depends, however, on the detection efficiency γ .

The most effective limit, $\gamma = 1$, is hypothetical but instructive. It corresponds to the situation in which all photons in the cavities can be measured with certainty, i.e., the cavities would have to be completely open. The ground state $|G\rangle$ is a superposition of any number of local and of nonlocal photon pairs. With perfect detection, the vacuum state can be uniquely identified (no detector clicks) and is discarded according to the measurement scheme. Any state which contains at least one local pair has photons of both polarizations on one side, and is discarded, too. The remaining states contain one

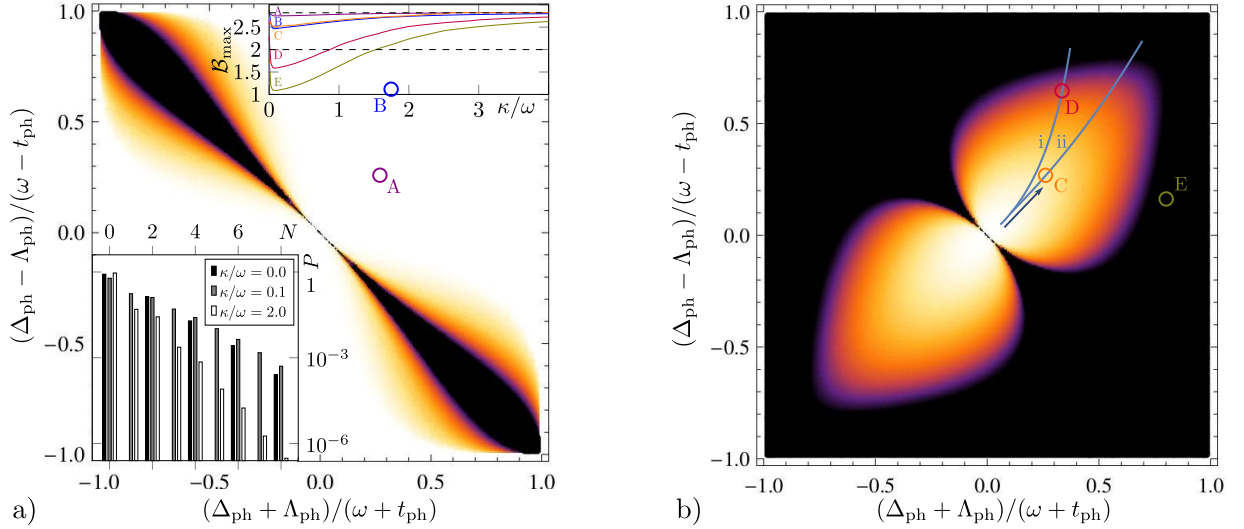


FIG. 2. Maximum violation of the CHSH Bell inequality depending on the local and nonlocal pair creation amplitudes Λ_{ph} and Δ_{ph} . In black regions entanglement cannot be detected, $\mathcal{B}_{\text{max}} \leq 2$. White regions correspond to $\mathcal{B}_{\text{max}} \geq 2\sqrt{2}$. a) Perfect detectors, $\gamma = 1$, isolate the contribution of a single nonlocal pair and entanglement is detectable for almost all parameters. Right inset: cavity losses affect \mathcal{B}_{max} (shown for different points A-E in the parameters space), possibly reducing it below the critical value 2 (lower dashed line). At high losses, however, all surviving coincidences are due to nonlocal pairs and \mathcal{B}_{max} approaches the two-particle maximum value $2\sqrt{2}$ (upper dashed line). Left inset: probabilities P to find N photons in the cavities at point B/D in the parameter space for different loss rates κ . At finite cavity losses, odd number states are populated, because photon pairs are broken up. b) Lossy detectors, $\gamma = 10^{-4}$ (see text), are able to detect entanglement if the admixture of local pairs is sufficiently small. The lines indicate the parameters obtained from the microscopic model if ECT is (i) as strong as CAR or (ii) half as strong as CAR. Following these lines in the direction of the arrow corresponds to different cavity detunings, $V_{\text{sd}} = \hbar\omega_0/e + \delta V_{\text{sd}}$, where δV_{sd} increases from $-1 \mu\text{eV}$ to $1 \mu\text{eV}$.

nonlocal pair, or, with an exponentially small amplitude, several nonlocal pairs. Hence \mathcal{B}_{max} is larger than the classical boundary 2 for almost any choice of parameters (Fig. 2a). In a realistic situation, we model the finite cavity resonance width by choosing $\gamma < 1$: even if the photodetectors themselves are flawless, during any coincidence interval Δt the probability for a single photon to leave its cavity is $1 - e^{-\kappa\Delta t} \gtrsim \gamma$, where we can express the loss rate $\kappa = (\omega + eV_{\text{sd}})/Q$ through the quality factor Q . Thus γ can safely be assumed to be larger than 10^{-4} [58]. In the Bell measurement, only one photon of a *local pair* might be detected and believed to belong to a *nonlocal pair*. At too large values of Λ_{ph} , \mathcal{B}_{max} is thus reduced below 2 and the entanglement of the nonlocal pairs – although present – cannot be detected anymore (Fig. 2b). Importantly, irrespective of γ , the Bell inequality is violated only if the nonlocal pairing amplitude Δ_{ph} is nonzero.

Cavity leakage.—Besides affecting the detection efficiency, cavity losses also modify the steady state. This influences the Bell measurement in two ways: entangled pairs can be broken up leaving behind unpaired photons. If their detection coincides with other photons, \mathcal{B}_{max} is reduced. On the other hand, \mathcal{B}_{max} is increased because the probability to have additional local pairs in the cavities is reduced. We model cavity losses with a Lindblad master equation [59] and solve it numerically [57] for the

steady state. When the loss rate κ dominates over the induced pairing amplitudes $|\Delta_{\text{ph}}|, |\Lambda_{\text{ph}}|$ (the most likely situation), in total \mathcal{B}_{max} is increased (Fig. 2a, inset).

To summarize, the Bell inequality is violated robustly over a broad range of configurations, but only if the nonlocal pairing amplitude Δ_{ph} is nonzero. Since Δ_{ph} is directly related to CAR (see below), observing $\mathcal{B}_{\text{max}} > 2$ is an experimental proof of coherent CP splitting.

Microscopic model.—In the remainder of the text, we derive the effective photonic Hamiltonian (1) microscopically. For the n-side, consider a double QD coupled to a SC lead, where the SC gap $\Delta = |\Delta|e^{i\phi}$ is the largest energy, $|\Delta| \gg |\epsilon_i|, k_B T$, with ϵ_i the spin-degenerate levels of the two QDs $i = 1, 2$, and T the temperature. We derive a Hamiltonian for the two QDs [57] to second order in the electron tunneling between the QDs and the lead,

$$H_e = \sum_{i\sigma} \epsilon_i d_{i\sigma}^\dagger d_{i\sigma} + \sum_{\sigma} \left[\tilde{\Delta} \sigma d_{1\sigma}^\dagger d_{2\sigma}^\dagger + \tilde{t} d_{1\sigma}^\dagger d_{2\sigma} + \text{h.c.} \right], \quad (5)$$

where $d_{i\sigma}$ annihilates electrons with spin $\sigma = \uparrow, \downarrow$ on QD i , and

$$\tilde{\Delta} = -\frac{\Gamma}{2} \frac{e^{-\frac{r}{\pi\xi} + i\phi}}{k_F r} \left[\sin(k_F r) + \frac{1 - \cos(k_F r)}{\pi k_F \xi} \right] \quad (6)$$

$$\tilde{t} = -\frac{\Gamma}{2} \frac{e^{-\frac{r}{\pi\xi}}}{k_F r} \left[\frac{\sin(k_F r)}{\pi k_F \xi} - (1 - \cos(k_F r)) \right], \quad (7)$$

where r is the distance between the tunneling points to QD 1 and QD 2 from the lead, $\xi = \hbar v_F / (\pi |\Delta|)$ is the lead coherence length and $\Gamma = 2\pi N(\epsilon_F) t_1 t_2$ is the normal state tunneling rate with t_i the amplitude for an electron to tunnel from the SC lead to QD i and N the normal density of states in the SC lead. We assume that double occupancy of a QD is forbidden by a large charging energy U_i [60]. On the p-side an equivalent Hamiltonian with $d_{i\sigma} \rightarrow h_{i\sigma} =: d_{i\bar{\sigma}}^{(\text{HH})\dagger}$ holds for the heavy holes (HH). Here, $d_{i\sigma}^{(\text{HH})\dagger}$ creates an electron with spin σ on QD i in the HH-band.

The parameters $\tilde{\Delta}$ and \tilde{t} capture the influence of the SC lead: $\tilde{\Delta}$ describes CAR, whereas \tilde{t} describes ECT between the QDs. Additionally, the onsite energies ϵ_i are renormalized. Optimal splitting requires $|\tilde{\Delta}| \gg |\tilde{t}|$, because ECT allows for sequential emission into the same cavity. This is realized in the limit of a small Fermi wave vector $k_F r \rightarrow 0$, which is achievable in principle, since k_F describes the semiconductor in which Δ is proximity-induced. For a more conservative estimate, if the separation of the tunnel contacts is large compared to the Fermi wavelength (but still smaller than ξ), it is evident that at best $|\tilde{\Delta}| \sim |\tilde{t}|$ can be realized. To be specific, we assume a large QD separation $k_F r \sim 10$, $r/(\pi\xi) \sim 0.5$ and $\Gamma = 500 \mu\text{eV}$ (Γ is limited by the gap in the SC, e.g., 1 meV for Nb). Then $\tilde{\Delta}$ and \tilde{t} are on the order of $15 \mu\text{eV}$. We note that because of the oscillating contributions in Eqs. (6) and (7) this may be fine-tuned via k_F in the SC lead.

The cavities are coupled to the electronic system by electron-hole recombination. In dipole approximation with the usual selection rules for HH using the rotating wave approximation,

$$H_I = \sum_{i\sigma} g_{i\sigma} e^{-ieV_{\text{sd}}t/\hbar} d_{i\sigma} h_{i\sigma} a_{i\sigma}^\dagger + \text{h.c.}, \quad (8)$$

with the annihilation operators for photons $a_{i\xi}$ emitted along the quantization axis of angular momentum and with radiative couplings $g_{i\xi}$ for cavity i and polarization ξ . For brevity we identify $\sigma = \uparrow$ with $\xi = R$ and $\sigma = \downarrow$ with $\xi = L$. The exponential accounts for the difference between the chemical potentials of n- and p-side set by the applied voltage bias. When it is gauged into the photon field $a \rightarrow e^{ieV_{\text{sd}}t/\hbar} a$, the complete photonic part of the Hamiltonian becomes

$$H_P = \sum_{i\xi} (\omega_0 - eV_{\text{sd}}) a_{i\xi}^\dagger a_{i\xi} + \sum_{i\sigma} g_{i\sigma} d_{i\sigma} h_{i\sigma} a_{i\sigma}^\dagger + \text{h.c.}, \quad (9)$$

with the cavity resonance frequency ω_0 .

Photoemission.—The ground state of the electronic system is a superposition of the empty state and the singlet state, $|0\rangle_e = c_{e,0}^0 | \rangle + c_{e,s}^0 |S\rangle$ with $| \rangle$ the empty dot, and $|S\rangle := 2^{-1/2} (d_{1\uparrow}^\dagger d_{2\downarrow}^\dagger - d_{1\downarrow}^\dagger d_{2\uparrow}^\dagger) | \rangle$ the nonlocal singlet.

The ground state energy is $E_e^0 = \epsilon - \sqrt{\epsilon^2 + 2|\tilde{\Delta}|^2}$, where

$\epsilon_{1,2} =: \epsilon \pm \delta$. The admixture of the singlet is controlled by the CAR amplitude $\tilde{\Delta}$, i.e., $|c_{e,s}^0| \rightarrow |c_{e,0}^0|$ as $|\tilde{\Delta}|/\epsilon \rightarrow \infty$. There are four relevant excited states, $|\sigma\pm\rangle_e = c_{e,1}^\pm |1\sigma\rangle + c_{e,2}^\pm |2\sigma\rangle$ with energies $E_e^\pm = \epsilon \pm \sqrt{\delta^2 + \tilde{t}^2}$, containing a single electron, which is delocalized due to ECT. Here, $|i\sigma\rangle := d_{i\sigma}^\dagger | \rangle$. The same applies to the hole states (Fig. 1). By electron-hole recombination and simultaneous emission of a photon as described by H_I , the n- and the p-side can both be excited from the ground state $|0\rangle_e |0\rangle_h$ into an excited state $|\sigma\mu\rangle_e |\bar{\sigma}\nu\rangle_h$, where $\mu, \nu = \pm$. Parity being protected, in order to go back to the ground state, this has to be followed by either a reabsorption, or by the emission of a second photon. This is possible because of the induced superconducting pairing, which breaks particle number conservation. If the excitation energies $\Delta E^{\mu\nu} = E_e^\mu + E_h^\nu - E_e^0 - E_h^0 \gtrsim \epsilon_e + \epsilon_h$, are larger than the cavity linewidth, this is a virtual process and photons are always emitted in pairs as desired. Importantly, the electron-hole system undergoes a closed cycle, so the entanglement is completely transferred [61] onto the photons [62]. To be specific, at $\tilde{\Delta} = 15 \mu\text{eV}$, a gate voltage needs to be applied to the QDs such that (i) $\epsilon = 30 \mu\text{eV}$ if $\tilde{t} = \tilde{\Delta}$, or such that (ii) $\epsilon = 20 \mu\text{eV}$ if $\tilde{t} = \tilde{\Delta}/2$. Here we assume $\delta = 0$, and electron-hole symmetry for simplicity, and use a linewidth on the order of 10 GHz, achievable for all common nanocavity flavors [63–66]. In principle, $\Delta E^{\mu\nu}$ can be made arbitrarily large (within the lead SC gap) to account for higher cavity losses by increasing ϵ . Since this, however, also reduces the CAR amplitude, it comes at the expense of a lower pair emission rate. With stronger CAR, $\tilde{\Delta} \gtrsim 30 \mu\text{eV}$, the QDs can even be brought into resonance with the leads, $\epsilon = 0$, to optimize the emission rate.

Quantitatively, the emission cycle is conveniently described with a standard Schrieffer-Wolff transformation [67], yielding the effective photonic model (1), with the pair emission amplitudes $\Delta_{\text{ph}}, \Lambda_{\text{ph}} \sim g(g/\Delta E)(\tilde{\Delta}/\epsilon)^2$. This corresponds to a total emission rate on the order of $10^{-3} g/\hbar$ if $\kappa > |\Delta_{\text{ph}}|, |\Lambda_{\text{ph}}|$. The full expressions are given in the Supplemental Material [57]. As expected, intercavity hopping t_{ph} and local pair injection Λ_{ph} vanish for $\tilde{t} = 0$. More importantly, even at finite \tilde{t} , we obtain effective parameters well within the region $\mathcal{B}_{\text{max}} > 2$. They are shown for the QD parameters (i) and (ii) at a QD-cavity coupling strength $g/(2\pi\hbar) = 3 \text{ GHz}$ [64, 65], in Fig. 2b.

In conclusion, we have investigated a coherent and continuous source of nonlocal photon pairs emitted from two optical QDs into two nanocavities embedded in a superconducting p-n junction. We showed that a Bell measurement can be used to investigate whether the light produced is entangled. Detection of these entangled photons would be a proof for spin coherence of Cooper pairs split over two QDs. The device does not require a driving scheme but only dc-voltages.

We thank J. C. Budich and F. Hassler for helpful discussions and acknowledge support from the EU-FP7 project SE2ND, No. 271554 and the DFG grant No. RE 2978/1-1.

SUPPLEMENTAL MATERIAL

Calculation of the detection probabilities

The detection probabilities $P_{\alpha\beta}^{\mu\nu}$ decompose into sums of expressions of the form

$$\begin{aligned} P_\eta &= \langle G | \eta_{1R}^{\dagger} \tilde{a}_{1R} \eta_{1L}^{\dagger} \tilde{a}_{1L} \eta_{2R}^{\dagger} \tilde{a}_{2R} \eta_{2L}^{\dagger} \tilde{a}_{2L} | G \rangle \\ &= \left| \eta_{1R}^{\dagger} \tilde{a}_{1R} \eta_{1L}^{\dagger} \tilde{a}_{1L} \eta_{2R}^{\dagger} \tilde{a}_{2R} \eta_{2L}^{\dagger} \tilde{a}_{2L} \right. \\ &\quad \exp \left[A(a_{1R}^{\dagger} a_{1L}^{\dagger} + a_{2R}^{\dagger} a_{2L}^{\dagger}) \right. \\ &\quad \left. \left. + B(a_{1R}^{\dagger} a_{2L}^{\dagger} + a_{1L}^{\dagger} a_{2R}^{\dagger}) \right] | \right|^2, \end{aligned} \quad (S1)$$

where $\eta_{i\xi} = 1 - \gamma$ or $\eta_{i\xi} = 1$. Employing the unitary transformation

$$\begin{aligned} \begin{pmatrix} \tilde{a}_{1R} \\ \tilde{a}_{1L} \\ \tilde{a}_{2R} \\ \tilde{a}_{2L} \end{pmatrix} &= U \begin{pmatrix} a_{1R} \\ a_{1L} \\ a_{2R} \\ a_{2L} \end{pmatrix}, \\ U &= \begin{pmatrix} \cos \alpha & -e^{i\phi} \sin \alpha & 0 & 0 \\ e^{-i\phi} \sin \alpha & \cos \alpha & 0 & 0 \\ 0 & 0 & \cos \beta & -e^{i\theta} \sin \beta \\ 0 & 0 & e^{-i\theta} \sin \beta & \cos \beta \end{pmatrix}, \end{aligned} \quad (S2)$$

together with the operator identity $x a^{\dagger} f(a^{\dagger}) = f(x a^{\dagger}) x a^{\dagger}$ [68], and using that $x a^{\dagger} | \rangle = | \rangle$, we rewrite

$$\begin{aligned} P_\eta &\propto \left| \exp \left[\frac{1}{2} (\tilde{a}_{1R}^{\dagger} \tilde{a}_{1L}^{\dagger} \tilde{a}_{2R}^{\dagger} \tilde{a}_{2L}^{\dagger}) D^T U^T M U D \begin{pmatrix} \tilde{a}_{1R}^{\dagger} \\ \tilde{a}_{1L}^{\dagger} \\ \tilde{a}_{2R}^{\dagger} \\ \tilde{a}_{2L}^{\dagger} \end{pmatrix} \right] | \right|^2 \\ &= \left| \exp \left[\frac{1}{2} \sum_{i1} \lambda_i b_i^{\dagger} b_i \right] | \right|^2, \end{aligned} \quad (S3)$$

where

$$D = \begin{pmatrix} \sqrt{\eta_{1R}} & 0 & 0 & 0 \\ 0 & \sqrt{\eta_{1L}} & 0 & 0 \\ 0 & 0 & \sqrt{\eta_{2R}} & 0 \\ 0 & 0 & 0 & \sqrt{\eta_{2L}} \end{pmatrix}, \quad (S4)$$

and

$$M = \begin{pmatrix} 0 & A & 0 & B \\ A & 0 & B & 0 \\ 0 & A & 0 & B \\ A & 0 & B & 0 \end{pmatrix}, \quad (S5)$$

and λ_i are the eigenvalues of $D^T U^T M U D$. The new bosons b_i are independent, so

$$P_\eta \propto \prod_{i=1}^4 \langle | e^{\frac{1}{2} \lambda_i^* b_i b_i} e^{\frac{1}{2} \lambda_i b_i^{\dagger} b_i^{\dagger}} | \rangle = \prod_{i=1}^4 (1 - |\lambda_i|^2). \quad (S6)$$

The last equality can be found by inserting the definition of the exponential as a series. If A and B have the same phase, it drops out in Eq. (S6).

Lindblad master equation

To study the influence of cavity losses, we solve the Lindblad master equation [59]

$$\dot{\rho} = \mathcal{L}\rho = -i[H, \rho] + \sum_{i\xi} \kappa \left(2a_{i\xi} \rho a_{i\xi}^{\dagger} - a_{i\xi}^{\dagger} a_{i\xi} \rho - \rho a_{i\xi}^{\dagger} a_{i\xi} \right) \quad (S7)$$

numerically for the steady state, $\dot{\rho}_{\text{steady}} = 0$. Here, ρ is the density matrix and \mathcal{L} is the Liouvillian superoperator, defined by the rightmost equality sign. The system Hamiltonian H is given by Eq. (1). The infinite-dimensional bosonic Hilbert space has to be truncated. We choose a cutoff at $N_{\text{max}} = 4$ bosons per mode ($i\xi$). The cutoff independence can be checked by comparing to a higher cutoff $N_{\text{max}} = 5$, comparing the solutions in a photon basis to the solution in a Bogoliubov basis and by comparing the $\kappa \rightarrow 0$ result with the exact calculation. In order to obtain the steady state we either explicitly propagate an arbitrary initial state in time until convergence or algebraically solve for the eigenvector of \mathcal{L} which has the smallest eigenvalue (always numerical 0).

Proximity effect

In this section we derive the pairing amplitudes $\tilde{\Delta}$ and \tilde{t} on the QDs, Eqs. (6) and (7). This is done most conveniently by performing a Schrieffer-Wolff transformation on an operator level via projection operators, following Ref. [44]. It applies independently to n- and p-side.

We consider the full device depicted in Fig. 1. Two optical QDs are coupled to a SC lead. Specifically,

$$H = H_0 + H_T \quad (S8)$$

$$\begin{aligned} H_0 &= \sum_{\mathbf{k}\sigma} E_{\mathbf{k}} \gamma_{\mathbf{k}\sigma}^{\dagger} \gamma_{\mathbf{k}\sigma} + \sum_{i\sigma} \epsilon_i d_{i\sigma}^{\dagger} d_{i\sigma} \\ &\quad + \sum_i U_i d_{i\uparrow}^{\dagger} d_{i\downarrow}^{\dagger} d_{i\downarrow} d_{i\uparrow} \end{aligned} \quad (S9)$$

$$H_T = \sum_{i\sigma} t_i d_{i\sigma}^{\dagger} \psi_{\sigma}(\mathbf{x}_i) + \text{h.c.}, \quad (S10)$$

where $E_{\mathbf{k}} = \sqrt{(\epsilon_{\mathbf{k}} - \mu)^2 + |\Delta|^2}$ is the dispersion of quasi-particles in the lead with gap energy $|\Delta|$ annihilated by γ ; ϵ_i and $U_i \rightarrow \infty$ are the onsite energy measured from

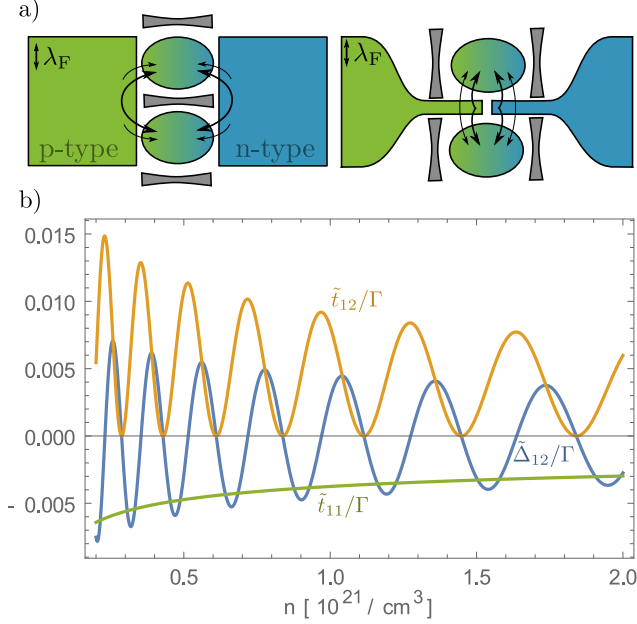


FIG. S1. a) Two different device geometries. Left panel: The tunnel contacts between the SC leads and QDs are separated by several Fermi wavelengths. ECT between the QDs is as strong as CP splitting. Right panel: Electrons can tunnel into both QDs from the same point in the SC leads. CP splitting dominates over ECT. b) Proximity induced amplitudes of CAR, $\tilde{\Delta}_{12}$, and ECT, \tilde{t}_{12} , and the renormalization of the on-site energy \tilde{t}_{11} at different carrier concentrations n . When optimizing the CP splitting amplitude, ECT cannot be neglected. The QDs are separated by $r = 100$ nm and the SC coherence length is $\xi = 200$ nm (arbitrarily chosen).

the chemical potential and the local Coulomb repulsion of electrons with spin $\sigma \in \{\uparrow, \downarrow\}$ on QD $i \in \{1, 2\}$ annihilated by d . We assume that there is only a single relevant level on each dot. Tunneling from point \mathbf{x}_i in the lead onto QD i has the amplitude $t_i \in \mathbb{R}$ (no magnetic fields). The operators ψ and γ are related through the Bogoliubov transformation $\psi_\sigma(\mathbf{x}) = \sum_{\mathbf{k}} e^{i\mathbf{k}\mathbf{x}} (u_{\mathbf{k}\sigma}^* \gamma_{\mathbf{k}\sigma} + \sigma v_{\mathbf{k}} \gamma_{-\mathbf{k}\bar{\sigma}}^\dagger)$, where the coherence factors obey $|v_{\mathbf{k}}|^2 = 1 - |u_{\mathbf{k}}|^2 = (1 - (\epsilon_{\mathbf{k}} - \mu)/E_{\mathbf{k}})/2$ and $v_{\mathbf{k}}^* u_{\mathbf{k}} = -|v_{\mathbf{k}}| |u_{\mathbf{k}}| e^{-i\phi}$ with the SC phase $\phi = \arg \Delta$.

Defining a set of projection operators,

$$P = \prod_{\mathbf{k}\sigma} (1 - \gamma_{\mathbf{k}\sigma}^\dagger \gamma_{\mathbf{k}\sigma}) \quad Q = 1 - P, \quad (\text{S11})$$

where P projects onto the lead ground state, the Hamiltonian can be written as

$$H_{\text{eff}} = PHP + PHQ(E - QHQ)^{-1}QHP \quad (\text{S12})$$

in the low-energy subspace [69]. Up to leading order in the tunneling amplitude t_i , this becomes

$$H_{\text{eff}} = H_0 + \sum_{ij\sigma} [\tilde{\Delta}_{ij} \sigma d_{i\sigma}^\dagger d_{j\bar{\sigma}}^\dagger + \text{h.c.} + \tilde{t}_{ij} d_{i\sigma}^\dagger d_{j\sigma}] \quad (\text{S13})$$

with the (C)AR amplitude

$$\tilde{\Delta}_{ij} = \sum_{\mathbf{k}} \frac{t_i t_j}{E_{\mathbf{k}}} \psi_{\mathbf{k}}(\mathbf{x}_i) \psi_{-\mathbf{k}}(\mathbf{x}_j) |u_{\mathbf{k}}| |v_{\mathbf{k}}| e^{i\phi}, \quad (\text{S14})$$

and the ECT amplitude

$$\tilde{t}_{ij} = - \sum_{\mathbf{k}} \frac{t_i t_j}{E_{\mathbf{k}}} \psi_{\mathbf{k}\sigma}(\mathbf{x}_i) \psi_{\mathbf{k}\sigma}^*(\mathbf{x}_j) (|u_{\mathbf{k}}|^2 - |v_{\mathbf{k}}|^2), \quad (\text{S15})$$

where we have used that $E_{\mathbf{k}} \sim |\Delta| \gg |\epsilon|$. Starting from Eq. (S12) higher-order terms can be included systematically, but they do not contain new effective processes, so it is safe to ignore them. Linearizing the bare spectrum of the lead $\epsilon_{\mathbf{k}}$ within the SC gap, the momentum summations can be performed as integrals over the density of states and we obtain $\tilde{\Delta} \equiv \tilde{\Delta}_{12}$ and $\tilde{t} \equiv \tilde{t}_{12}$ as given in Eqs. (6) and (7). The renormalization of the onsite energies by \tilde{t}_{ii} is obtained as the $r \rightarrow 0$ limit of Eq. (7), but can be absorbed into ϵ . The dependency of the amplitudes on the carrier concentration is illustrated in Fig. S1b.

Parameters of the effective model

Decoupling the low energy sector (the electron-hole system is in its ground state) from the high energy sector (the electron-hole system is in any other state) up to second order in $g_{i\xi}$, following, e.g., Ref. [70], we find

$$H_{\text{ph}} = \sum_{i\xi} (\omega_0 - eV_{\text{sd}}) a_{i\xi}^\dagger a_{i\xi} + \sum_{ij\xi} M_{ij\xi} a_{i\xi}^\dagger a_{j\xi} + \sum_{ij\xi} \frac{\tilde{M}_{ij\xi}}{2} a_{i\xi} a_{j\xi} + \text{h.c.}, \quad (\text{S16})$$

where

$$M_{ij\xi} = g_{i\xi} g_{j\xi}^* \sum_{\mu\nu=\pm} \left(\frac{|c_{e,0}^0|^2 |c_{h,0}^0|^2 c_{e,i}^\mu c_{e,j}^{\mu*} c_{h,i}^\nu c_{h,j}^{\nu*}}{(\omega_0 - eV_{\text{sd}}) - \Delta E^{\mu\nu}} - \frac{1}{4} \frac{|c_{e,s}^0|^2 |c_{h,s}^0|^2 c_{e,i}^{\mu*} c_{e,j}^\mu c_{h,i}^{\nu*} c_{h,j}^\nu}{(\omega_0 - eV_{\text{sd}}) + \Delta E^{\mu\nu}} \right) \quad (\text{S17})$$

$$\tilde{M}_{ij\xi} = g_{i\xi}^* g_{j\xi} \sum_{\mu\nu=\pm} \frac{c_{e,s}^{0*} c_{e,0}^0 c_{h,s}^{0*} c_{h,0}^0 c_{h,i}^{\nu*} c_{h,j}^\nu c_{e,i}^{\mu*} c_{e,j}^\mu}{(\Delta E^{\mu\nu})^2 - (\omega_0 - eV_{\text{sd}})^2}. \quad (\text{S18})$$

The amplitudes c are obtained exactly by diagonalizing the 2×2 blocks of the effective QD Hamiltonian (5). At symmetric gating, $\delta = 0$, as discussed in the main text the excited state amplitudes $c_{e/h,i}^{\pm}$ are on the order of 1 and the ground state amplitudes fulfill $|c_{e/h,s}^{0*} c_{e/h,0}^0| = |\tilde{\Delta}|/(2|\epsilon|) + \mathcal{O}(|\tilde{\Delta}|^2/\epsilon^2)$. With two identical QDs, two identical cavities, and polarization independent radiative couplings g , Eq. (S16) is equivalent to the effective photonic model (1), with $\omega = \omega_0 - eV_{sd} + M_{i=j}$, $t_{ph} = M_{i \neq j}$, $\Lambda_{ph} = \tilde{M}_{i=j}$ and $\Delta_{ph} = \tilde{M}_{i \neq j}$.

-
- [1] M. A. Nielsen and I. L. Chuang, *Quantum Computation and Quantum Information* (Cambridge University Press, Cambridge, England, 2000).
 - [2] M.-S. Choi, C. Bruder, and D. Loss, Phys. Rev. B **62**, 13569 (2000).
 - [3] J. Torrès and T. Martin, Eur. Phys. J. B **12**, 319 (1999).
 - [4] G. Falci, D. Feinberg, and F. W. J. Hekking, Europhys. Lett. **54**, 255 (2001).
 - [5] P. Recher, E. V. Sukhorukov, and D. Loss, Phys. Rev. B **63**, 165314 (2001).
 - [6] G. Lesovik, T. Martin, and G. Blatter, Eur. Phys. J. B **24**, 287 (2001).
 - [7] P. Recher and D. Loss, Phys. Rev. B **65**, 165327 (2002).
 - [8] C. Bena, S. Vishveshwara, L. Balents, and M. P. A. Fisher, Phys. Rev. Lett. **89**, 037901 (2002).
 - [9] P. Recher and D. Loss, Phys. Rev. Lett. **91**, 267003 (2003).
 - [10] A. Levy Yeyati, F. S. Bergeret, A. Martin-Rodero, and T. M. Klapwijk, Nat. Phys. **3**, 455 (2007).
 - [11] J. Cayssol, Phys. Rev. Lett. **100**, 147001 (2008).
 - [12] K. Sato, D. Loss, and Y. Tserkovnyak, Phys. Rev. Lett. **105**, 226401 (2010).
 - [13] L. Hofstetter, S. Csonka, J. Nygård, and C. Schönenberger, Nature (London) **461**, 960 (2009).
 - [14] L. G. Herrmann, F. Portier, P. Roche, A. Levy Yeyati, T. Kontos, and C. Strunk, Phys. Rev. Lett. **104**, 026801 (2010).
 - [15] A. Das, Y. Ronen, M. Heiblum, D. Mahalu, A. V. Kretinin, and H. Shtrikman, Nat. Commun. **3**, 1165 (2012).
 - [16] J. Wei and V. Chandrasekhar, Nature Phys. **6**, 494 (2010).
 - [17] S. Kawabata, J. Phys. Soc. Jpn. **70**, 1210 (2001).
 - [18] N. M. Chtchelkatchev, G. Blatter, G. B. Lesovik, and T. Martin, Phys. Rev. B **66**, 161320 (2002).
 - [19] P. Samuelsson, E. V. Sukhorukov, and M. Büttiker, Phys. Rev. Lett. **91**, 157002 (2003).
 - [20] C. W. J. Beenakker, C. Emary, M. Kindermann, and J. L. van Velsen, Phys. Rev. Lett. **91**, 147901 (2003).
 - [21] P. Samuelsson, E. V. Sukhorukov, and M. Büttiker, Phys. Rev. Lett. **92**, 026805 (2004).
 - [22] O. Sauret, T. Martin, and D. Feinberg, Phys. Rev. B **72**, 024544 (2005).
 - [23] W. Chen, R. Shen, L. Sheng, B. G. Wang, and D. Y. Xing, Phys. Rev. Lett. **109**, 036802 (2012).
 - [24] B. Braunecker, P. Burset, and A. Levy Yeyati, Phys. Rev. Lett. **111**, 136806 (2013).
 - [25] G. Burkard, D. Loss, and E. V. Sukhorukov, Phys. Rev. B **61**, R16303 (2000).
 - [26] J. C. Egues, G. Burkard, and D. Loss, Phys. Rev. Lett. **89**, 176401 (2002).
 - [27] G. Burkard and D. Loss, Phys. Rev. Lett. **91**, 087903 (2003).
 - [28] X. Hu and S. Das Sarma, Phys. Rev. B **69**, 115312 (2004).
 - [29] P. Samuelsson, E. V. Sukhorukov, and M. Büttiker, Phys. Rev. B **70**, 115330 (2004).
 - [30] J. C. Egues, G. Burkard, D. S. Saraga, J. Schliemann, and D. Loss, Phys. Rev. B **72**, 235326 (2005).
 - [31] V. Giovannetti, D. Frustaglia, F. Taddei, and R. Fazio, Phys. Rev. B **74**, 115315 (2006).
 - [32] P. San-Jose and E. Prada, Phys. Rev. B **74**, 045305 (2006).
 - [33] F. Mazza, B. Braunecker, P. Recher, and A. Levy Yeyati, Phys. Rev. B **88**, 195403 (2013).
 - [34] A. Schroer, B. Braunecker, A. Levy Yeyati, and P. Recher, Phys. Rev. Lett. **113**, 266401 (2014).
 - [35] S. J. Freedman and J. F. Clauser, Phys. Rev. Lett. **28**, 938 (1972).
 - [36] A. Aspect, J. Dalibard, and G. Roger, Phys. Rev. Lett. **49**, 1804 (1982).
 - [37] G. Weihs, T. Jennewein, C. Simon, H. Weinfurter, and A. Zeilinger, Phys. Rev. Lett. **81**, 5039 (1998).
 - [38] J. S. Bell, Physics **1** (1964).
 - [39] J. F. Clauser, M. A. Horne, A. Shimony, and R. A. Holt, Phys. Rev. Lett. **23**, 880 (1969).
 - [40] E. Hanamura, Phys. Status Solidi B **234**, 166 (2002).
 - [41] Y. Asano, I. Suemune, H. Takayanagi, and E. Hanamura, Phys. Rev. Lett. **103**, 187001 (2009).
 - [42] H. Sasakura, S. Kuramitsu, Y. Hayashi, K. Tanaka, T. Akazaki, E. Hanamura, R. Inoue, H. Takayanagi, Y. Asano, C. Hermannstädter, H. Kumano, and I. Suemune, Phys. Rev. Lett. **107**, 157403 (2011).
 - [43] I. Suemune, T. Akazaki, K. Tanaka, M. Jo, K. Uesugi, M. Endo, H. Kumano, E. Hanamura, H. Takayanagi, M. Yamanishi, and H. Kan, Jpn. J. Appl. Phys. **45**, 9264 (2006).
 - [44] P. Recher, Y. V. Nazarov, and L. P. Kouwenhoven, Phys. Rev. Lett. **104**, 156802 (2010).
 - [45] F. Hassler, Y. V. Nazarov, and L. P. Kouwenhoven, Nanotechnology **21**, 274004 (2010).
 - [46] P. Baireuther, P. P. Orth, I. Vekhter, and J. Schmalian, Phys. Rev. Lett. **112**, 077003 (2014).
 - [47] A. Hayat, H.-Y. Kee, K. S. Burch, and A. M. Steinberg, Phys. Rev. B **89**, 094508 (2014).
 - [48] F. Godschalk, F. Hassler, and Y. V. Nazarov, Phys. Rev. Lett. **107**, 073901 (2011).
 - [49] F. Godschalk and Y. V. Nazarov, Phys. Rev. B **87**, 094511 (2013).
 - [50] F. Godschalk and Y. V. Nazarov, Phys. Rev. B **89**, 104502 (2014).
 - [51] O. Gywat, G. Burkard, and D. Loss, Phys. Rev. B **65**, 205329 (2002).
 - [52] V. Cerletti, O. Gywat, and D. Loss, Phys. Rev. B **72**, 115316 (2005).
 - [53] J. C. Budich and B. Trauzettel, Nanotechnology **21**, 274001 (2010).
 - [54] S. E. Nigg, R. P. Tiwari, S. Walter, and T. L. Schmidt, arxiv:1411.3945.
 - [55] W. Vogel, D.-G. Welsch, and S. Wallentowitz, *Quantum Optics An Introduction* (WILEY-VCH Verlag, Berlin, 2001).

- [56] V. C. Vivoli, P. Sekatski, J. D. Bancal, C. C. W. Lim, B. G. Christensen, A. Martin, R. T. Thew, H. Zbinden, N. Gisin, and N. Sangouard, arxiv:1405.1939.
- [57] See Supplemental Material for further details.
- [58] For this estimate, we assume a worst-case set of parameters: a high quality factor $Q = 10^6$, infrared light $f = 10$ THz and a short coincidence interval $\Delta t = 1$ ps.
- [59] C. W. Gardiner and P. Zoller, *Quantum Noise* (Springer, Berlin, 2000).
- [60] At finite Coulomb repulsion $U < |\Delta|$, the electron-hole system can be diagonalized perturbatively in $1/U$ or numerically. This substantially complicates the notation while not producing any new effects, so we focus on the (experimentally more relevant) case $U \gg |\Delta|$, in which ECT between the QDs via the SC lead is the dominant source of local photon pairs.
- [61] M. Titov, B. Trauzettel, B. Michaelis, and C. W. J. Beenakker, *New Journal of Physics* **7**, 186 (2005).
- [62] Because of parity conservation we expect the photons to be entangled even if the cavity linewidth κ is larger than $\Delta E^{\mu\nu}$ (but smaller than Δ in the SC leads and U). This, however, leads to a different regime in which single photons can be emitted sequentially, and requires a separate calculation.
- [63] K. Hennessy, A. Badolato, M. Winger, D. Gerace, M. Atature, S. Gulde, S. Falt, E. L. Hu, and A. Imamoglu, *Nature (London)* **445**, 896 (2007).
- [64] K. Srinivasan and O. Painter, *Nature* **450**, 862 (2007).
- [65] V. Loo, L. Lanco, A. Lematre, I. Sagnes, O. Krebs, P. Voisin, and P. Senellart, *Appl. Phys. Lett.* **97**, 241110 (2010).
- [66] R. Ohta, Y. Ota, M. Nomura, N. Kumagai, S. Ishida, S. Iwamoto, and Y. Arakawa, *Appl. Phys. Lett.* **98**, 173104 (2011).
- [67] J. R. Schrieffer and P. A. Wolff, *Phys. Rev.* **149**, 491 (1966).
- [68] P. Sekatski, B. Sanguinetti, E. Pomarico, N. Gisin, and C. Simon, *Phys. Rev. A* **82**, 053814 (2010).
- [69] F. H. L. Essler, H. Frahm, F. Göhmann, A. Klümper, and V. E. Korepin, *The One-Dimensional Hubbard Model* (Cambridge University Press, 2005).
- [70] R. Winkler, *Spin-Orbit Coupling Effects in Two-Dimensional Electron and Hole Systems* (Springer-Verlag, 2003).